Collective motion from local attraction

Daniel Strömbom

Mathematics Department, Uppsala University, Box 480, 751 06 Uppsala, Sweden

ARTICLE INFO

ABSTRACT

Many animal groups, for example schools of fish or flocks of birds, exhibit complex dynamic patterns while moving cohesively in the same direction. These flocking patterns have been studied using self-propelled particle models, most of which assume that collective motion arises from individuals aligning with their neighbours. Here, we propose a self-propelled particle model in which the only social force between individuals is attraction. We show that this model generates three different phases: swarms, undirected mills and moving aligned groups. By studying our model in the zero noise limit, we show how these phases depend on the relative strength of attraction and individual inertia. Moreover, by restricting the field of vision of the individuals and increasing the degree of noise in the system, we find that the groups generate both directed mills and three dynamically moving, 'rotating chain' structures. A rich diversity of patterns is generated by social attraction alone, which may provide insight into the dynamics of natural flocks.

1. Introduction

A number of models of flocking, often referred to as self-propelled particle (SPP) models, have been constructed and analysed in recent years (Aoki, 1982; Huth and Wissel, 1991; Vicsek et al., 1995; Grégorie et al., 2003; Czirók et al., 1997; Czirók and Vicsek, 2000; Couzin et al., 2002; Czirók et al., 1999; D'Orsogna et al., 2006; Wood and Ackland, 2007; Romanczuk et al., 2008; Lukeman et al., 2009). The main difference between the different models is the form of the local interaction rule and how neighbouring particles affect each other. The interaction rule typically depends on a few directional components, from average orientation of neighbours alone in Vicsek et al. (1995) to orientation, attraction and repulsion in e.g. Aoki (1982), Huth and Wissel (1991) and Couzin et al. (2002). Typically, the distance between neighbours determines whether they are attracted, repelled or aligned to each other. For a recent review, see Yates et al. (2010).

All the above models assume that individuals change their orientation in response to the orientation of, at least some, of their neighbours. This explicit local alignment rule then produces collective motion in the same direction of large numbers of individuals on a global scale (Grégorie et al., 2003; Vicsek et al., 1995). So do all organisms exhibiting collective motion measure local alignment? We expect the answer to vary depending on the species studied. For example, locusts interact through cannibalistic interactions, where locusts chase those in front and escape those behind (Bazazi et al., 2008; Hale, 2008), but nonetheless produce highly aligned groups (Buhl et al., 2006). Starling flocks

also exhibit co-ordinated collective motion, but as yet there is little information about what determines an individual's propensity to change direction (Ballerini et al., 2008). Some fish species, for example Saithe, do appear to match their direction to that of their neighbours (Partridge, 1981). However, Partridge and Pitcher (1980) found that disabling the lateral line, otherwise used by fish to obtain directional information, did not reduce the degree to which neighbouring fishes direction was correlated. Szabó et al. (2006) have shown that even simple tissue cells from the scales of gold fish can align at high densities, although it is highly unlikely that they achieve this by explicitly measuring the directions of their neighbours. In general, the fact that we see groups move collectively or even that we see individuals in a group locally aligned does not imply that they are using a specific local alignment rule.

Removing the alignment term from SPP models leaves us with only attraction and repulsion. One possibility is that an asymmetrical combination of attraction to individuals in front and repulsion from those behind can produce a co-ordinated moving cluster. Such a phenomena is seen in the optimal velocity model (Bando et al., 1995; Sugiyama, 2008) and an 'escape and pursuit' model (Romanczuk et al., 2008). Here we concentrate on a further simplification in which we use just one term for social interactions, namely local attraction. SPP models with global attraction as the only interaction produce a range of dynamic structures, some of which produce dynamic moving patterns (Mikhailov and Zanette, 1999; Erdmann et al., 2005; Ebeling and Schimansky-Geier, 2008). Here we concentrate on a minimal model in which we use local attraction.

For a model with only attraction modified classical mechanics can be applied to analyse the model. One advantage of this approach is that it allows us to determine analytically for which

E-mail address: strombom@math.uu.se

dynamic shapes alignment is or is not required. While the model we propose is simpler than those suggested previously, we will show that not only can attraction alone produce many of the patterns seen in models with alignment, but it produces a rich variety of complex dynamic patterns of its own.

2. The model

The general setup of our model is the same as in the SPP models discussed in the introduction. N particles move within an $L \times L$ two dimensional space with periodic boundary conditions (i.e. on a torus). Initially the particles are given random positions and headings. The position of particle i at time t is denoted by $P_{i,t}$, while the unit vector indicating direction is denoted $\hat{D}_{i,t}$. On each time step each particle interacts with neighbouring particles located within a distance of R. The only social interaction in the model is an attraction to the centre of mass of the neighbouring particles, and $\hat{C}_{i,t}$ is used to denote normalised direction toward this centre of mass. The parameters d,c,e are used to set the relative strength's of the forces acting on a particle. d determines the directional inertia of the particle, or its tendency to continue in its previous direction. c is the particle's attraction to the centre of mass of its neighbouring particles ($\hat{C}$), while e determines the degree of random motion. δ is the (average) speed of the particles. Noise is incorporated into the model in two ways. Firstly, the directional error is given by $\hat{\varepsilon}_{i,t} = [\cos\theta_{i,t}, \sin\theta_{i,t}]$, where $\theta_{i,t}$ taken from a normal distribution with mean 0 and standard deviation 1. Secondly, variation in speed is modelled by a random variable $\zeta_{i,t}$ taken from a uniform distribution with range $[-\eta/2, \eta/2]$.

At each time step a new direction and position for each particle is calculated as follows. Particle i's heading at time $t+1$ given the state at time t is

$$D_{i,t+1} = d\hat{D}_{i,t} + c\hat{C}_{i,t} + e\hat{\varepsilon}_{i,t}, \tag{1}$$

which is then normalised to give $\hat{D}_{i,t+1}$ and the new position is calculated by

$$P_{i,t+1} = P_{i,t} + \delta(1 + \zeta_{i,t})\hat{D}_{i,t+1}. \tag{2}$$

In some simulations the particles cannot detect other particles in a region behind them, defined to be a blind angle β. Specifically, particle i at position P_i with normalised heading $\hat{D}_i$ will not be influenced by particle j at position P_j if

$$\left| \arccos\left(\frac{P_iP_j \cdot \hat{D}_i}{|P_iP_j|} \right) \right| < \frac{\beta}{2}.$$

Appropriate modifications were made in all calculations to account for periodic boundary conditions.

As a test of model robustness, two different heading/position update schemes are employed: sequential random and simultaneous. Sequential random is where the particles update their heading/position sequentially in each time step and the order in which they do so is random from one time step to the next. Simultaneous is where at each time step each particle calculates its heading/position based on the neighbour data from the previous time step.

We use measures to analyse the outcome of our simulations. First the well-known alignment (Vicsek et al., 1995) defined by

$$\alpha = \frac{1}{N} \sqrt{ \left(\sum_{i=1}^{N} \cos\theta_i \right)^2 + \left(\sum_{i=1}^{N} \sin\theta_i \right)^2 }, \tag{3}$$

where θ_i is the directional angle of particle i. It measures the extent to which the particles are moving in the same direction. It ranges from 0 to 1, with 1 if all particles are moving in the same direction. The second measure is an approximation of the spatial extent of the group, and is defined by

$$A = (\max(x) - \min(x))(\max(y) - \min(y)), \tag{4}$$

where x and y are the sets of x- and y-coordinates of all the particles. The measure gives the area of the smallest square containing the group and can range from 0, where all particles occupy a single point, to L^2, where the particles range over the entire space.

3. Results

Before presenting simulations of our model we first derive the group structure in terms of the parameters c and d in the error-free case ($e = 0$ and $\eta = 0$) and no blind angle ($\beta = 0$). We now show that three group structures are possible: swarms, undirected mills and moving aligned groups. Fig. 1 shows the basic geometry of how particles are influenced by attraction to centre of mass and directional inertia. The attraction to the centre of mass is independent of the number of neighbours, thus the centre of mass of a particle established by one neighbour particle is indistinguishable from the centre of mass established by many neighbours. Hence we can, for each particle in each time step, consider the interaction as a two body problem, where the bodies are the particle itself and the centre of mass of its neighbouring particles.

To get the criterion for the group structure to be a circle recall the dynamics of circular motion from elementary physics. In the discrete case assuming constant speed c is given by

$$c = \frac{d\delta}{r}, \tag{5}$$

where r is the radius of the circle and δ is the displacement (see Appendix A for a derivation of (5)). Now, in the continuous case ($r = d^2/c$) and with infinite interaction range, given any pair of d and c the particles will form a circle of radius r or collapse to a point. In the discrete case with finite interaction radius R there are two cut-offs. If the diameter $2r$ of the potential circle is larger than R then the centre of mass detected by the particle will not be the centre of mass of the potential circle and hence no circle will form. Thus for circle formation we require
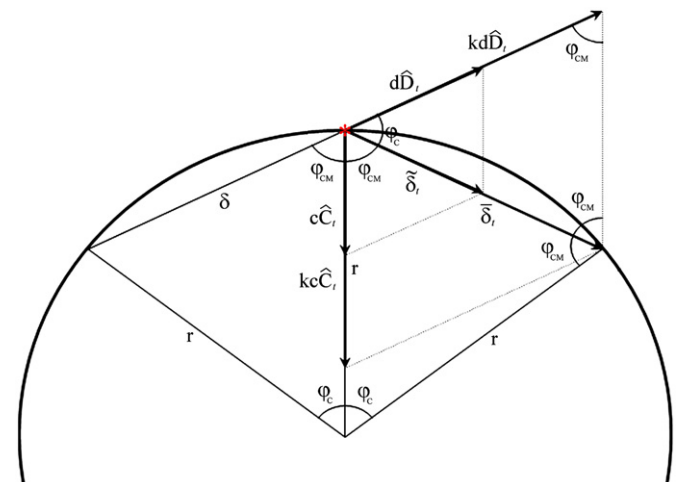
$$R \geq 2r. \tag{6}$$

Fig. 1. Figure showing the geometry of particle located at ✳ moving clock-wise on a mill of radius r in terms of the model parameters. The parameters c and d determines the heading $\tilde{\delta}_t$ and this is then scaled by $k = \delta/|\tilde{\delta}_t|$ to produce the directional vector $\bar{\delta}_t$ of length δ. Of particular interest are the angles φ_C, between the previous and the current heading, and φ_{CM}, between the current heading and a vector pointing towards the centre of mass.

To obtain an upper limit on the main parameter d/c for circle formation we combine (6) with (5) and get

$$\frac{d}{c} \leq \frac{R}{2\delta}. \tag{7}$$

We call any circle which forms in this manner an *undirected mill*, in order to emphasise that particles can move in either direction around the centre of mass.

For a lower limit on undirected mill formation note that a particle on a circle at most can turn straight toward the centre of mass. The angle between previous and current direction for motion on a circle is given by

$$\varphi_C = 2\arcsin\left(\frac{c}{2d}\right). \tag{8}$$

(see appendix A). The angle between the previous direction and a vector pointing to the centre of mass by ψ. Then as the particle can never turn more than π if on a circle we must always have

$$\pi \geq \psi = \arcsin\left(\frac{\delta}{R}\right) + \frac{\pi}{2}. \tag{9}$$

As $2\arcsin(x)$ is strictly increasing and the particle at most can turn to go straight toward the centre of mass we have with (7) that

$$\frac{\pi}{2} + \arcsin\left(\frac{\delta}{R}\right) \geq 2\arcsin\left(\frac{c}{2d}\right) \geq 2\arcsin\left(\frac{\delta}{R}\right). \tag{10}$$

Manipulating this gives

$$\sqrt{\frac{R}{2(R+\delta)}} \leq \frac{d}{c} \leq \frac{R}{2\delta}, \tag{11}$$

which is the main condition for undirected mill formation.

So what about the swarms and aligned groups? Define φ_R to be the actual angle between the previous and current direction. If $\varphi_R > \varphi_C$ then each particle at each time step will move into the potential circle. Once inside they cannot move out and collectively comprising a *swarm*. If $\varphi_R < \varphi_C$ then each particle on the potential circle will move outside of it. If close enough together and facing in a sufficiently similar direction, when leaving the circle, two or more particles will keep in contact with each other. Over time the distance to each other will decrease (at a rate depending on d/c) in a damped oscillation-type fashion and as the distance decrease their directions converge and a *cohesively moving aligned group* will form.

Simulations in the error-free case without blind angle reflect the above analysis. Fig. 2 shows three simulation outcomes corresponding to the three group types. The measures of alignment α (Eq. (3)) and area A (Eq. (4)) can now be used to quantify the form of these groups over different values of the model parameters, δ, d and c. A cohesively moving aligned group should have high alignment and low area. A mill is group where all particles are moving in a circular path around a common centre and should thus be characterized by low alignment and constant area, $4r^2$, where r is the radius of the mill. Finally a swarm is a group with low and varying alignment and area approximately equal to the smallest circle that can form.

Fig. 3 shows how alignment and area depend on the model parameter values. Comparing simulations directly with the
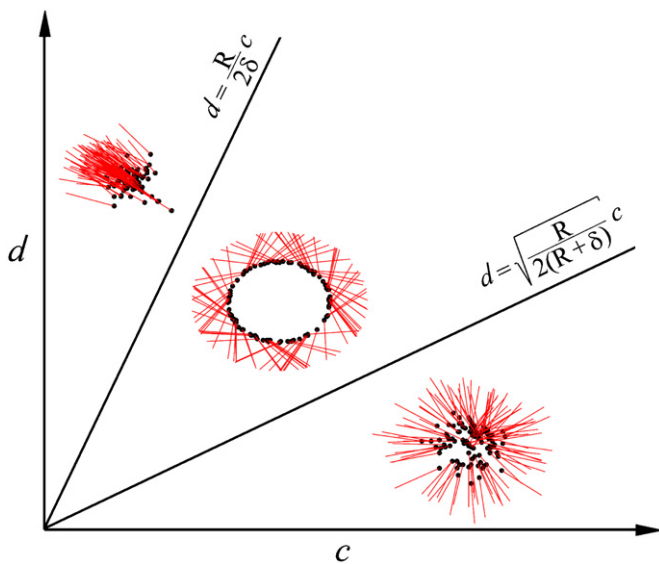

Fig. 2. Schematic phase diagram in the d–c plane indicating the phase formed by typical examples of the structures taken from simulations. In clockwise order, cohesively moving aligned group (dynamic parallel motion), mill and swarm. Each black dot is a particle and the rod attached to it indicate the direction of travel.
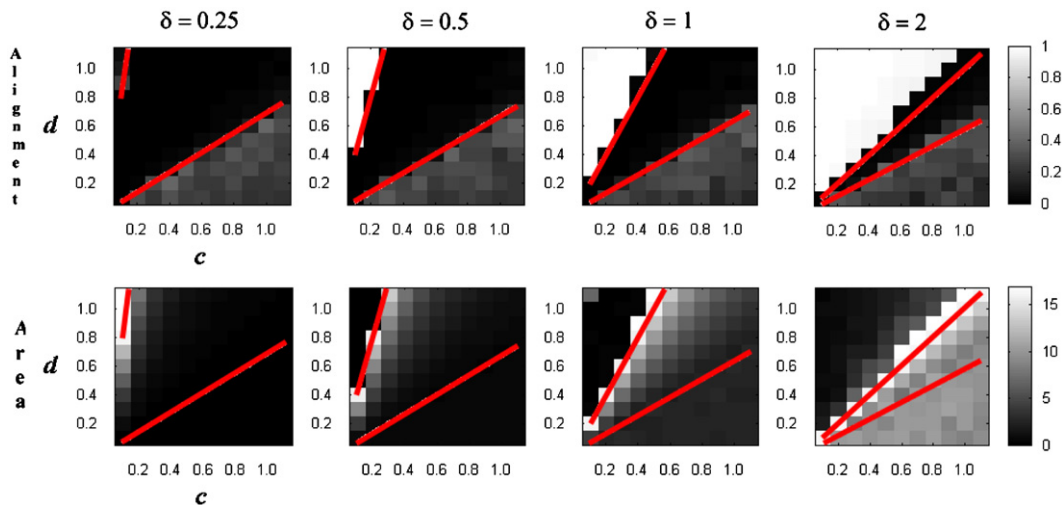

Fig. 3. The alignment and area for combinations of d and c in 0.1 to 1.1 from simulations with $R=4$ and δ being 0.25, 0.5, 1 and 2 (from left to right). ($L=10, N=50, t=5000, e=\eta=0$). The white lines correspond to the limits, cf Fig. 2. Areas exceeding 17 (no single typical structure has formed on the $L \times L$ square) are set to 17 in order to enhance detail in the important parts of the plot.

analytically predicted lines

$$d = \sqrt{\frac{R}{2(R+\delta)}}c \quad \text{and} \quad d = \frac{R}{2\delta}c,$$

we see that these accurately predict transitions between different structures. The typical structures are stable in the presence of noise, $e > 0$. Increasing the noise simply makes the structure less dense. The cohesively moving aligned group becomes wider and the mill goes from being a thin circle to an annulus and eventually a disc. Fig. 4 shows typical examples as we increase noise.

Introducing a blind angle ($\beta > 0$) has a dramatic effect on the types of collective patterns observed in model simulations. Firstly, particles are more likely to form a mill in which a clear majority travel round the circle in the same direction (Fig. 5a). These directed mills typically occur when the front of an elongated moving dynamic group turns sufficiently far round so as to meet its tail. This shape then stabilises into a circular mill.

In addition to the directed mill, we see the formation of three new structures in simulations, which we call *rotating chains*. In these rotating chains the individuals move on a closed curve with zero (Fig. 5b), one (Fig. 5c) or two (Fig. 5d) proper self-intersections. The chains exhibit highly dynamic patterns. Those with zero or two proper intersections are typically rotating around an axis which changes slowly over time (see videos 1 and 2). The structure with one intersection is most striking in that it exhibits a high degree of collective motion. In all cases it moves straight in one direction (see video 3), while internally rotating round a figure of eight. Letting the particles use the interaction rule with probability p and continue in the previous direction with probability $1-p$ the displacement δ can be decreased but still allow for a sizeable structure (see video 4 where $p=0.1$ and $\delta=0.025$).

All dynamic shapes formed when particles have a blind angle and these are stable in the presence of a high degree of noise. The structures shown in Fig. 5 were generated with both angular noise and propulsion noise. To investigate the robustness of
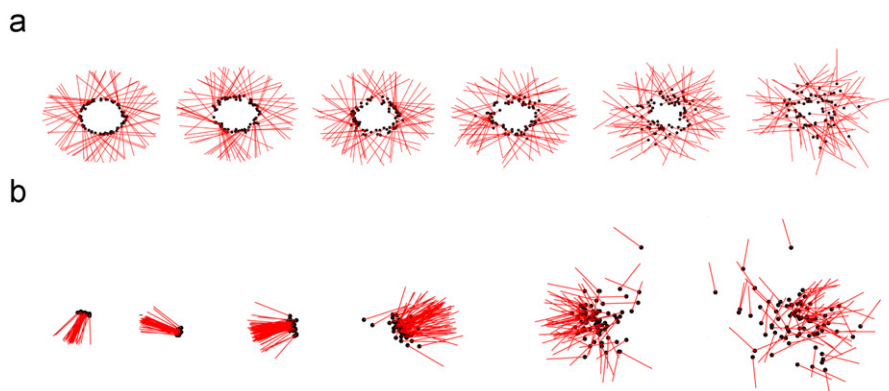

Fig. 4. (a) Shows the effect of increasing e through 0.05, 0.1, 0.15, 0.2, 0.3, 0.4 on the mill phase ($N=80, L=10, R=4, \delta=0.5, a=1, c=1, \eta=0$). (b) The effect on the dynamic parallel phase when increasing the e through 0, 0.1, 0.5, 1, 1.5, 2 with the other parameters as in (a).
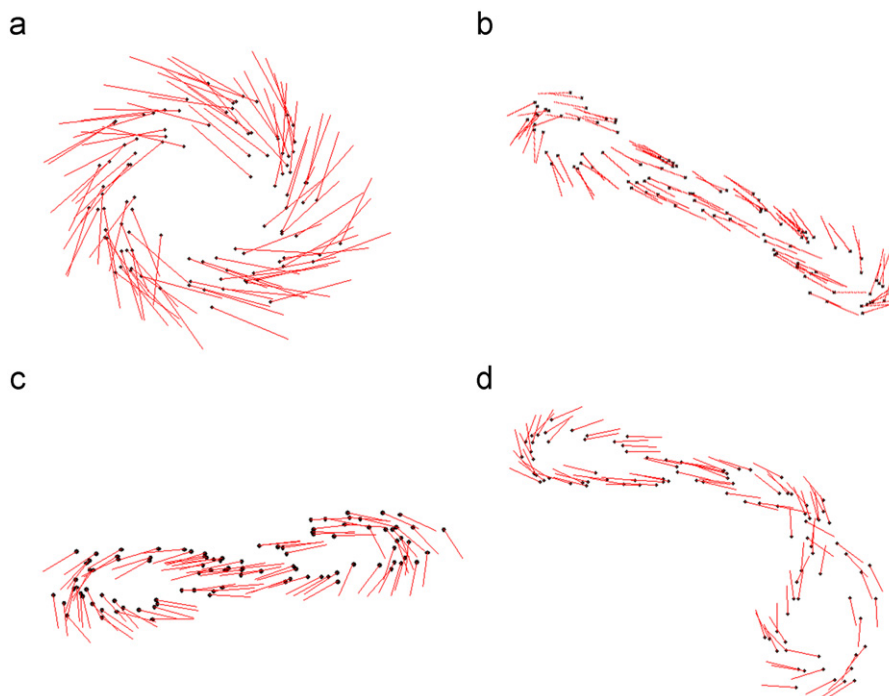

Fig. 5. Additional structures appearing when a blind angle is introduced illustrated in a situation with plenty of both angular and propulsion noise. From left to right: (a) a fully oriented mill ($d=1.5$) and rotating chains with (b) zero ($d=2.6$), (c) one ($d=3.2$) and (d) two self-intersections ($d=3.0$). The other parameters being $L=40$, $N=100$, $R=4$, $\delta=0.5$, $c=1$, $e=0.2$, $\eta=0.5$ and $\beta=2$ in all four cases.
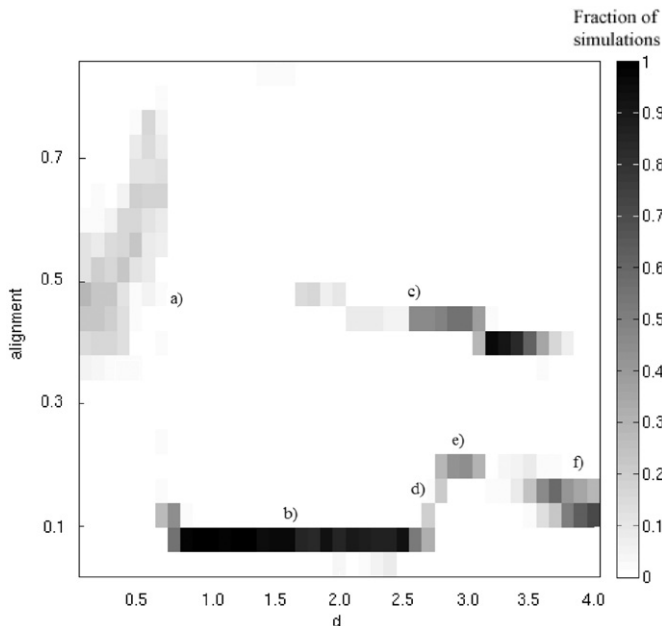
Fig. 6. Proportion of runs resulting in an alignment value within a certain bin versus d for fixed $c=1$ in a situation with large blind angle and noise of both types. d was increased incrementally by 0.1 from 0 to 4. For each d 100 independent runs over 10 000 time steps was conducted and the alignment was averaged over the last 1000 time steps in each. The other parameters was $L=40$, $N=100$, $R=4$, $\delta=0.5$, $d=2$, $c=1$, $e=0.2$, $\eta=0.5$ and $\beta=2$. Through observation we established the correspondence between this plot and the structures in Fig. 5. (a) Typically several dynamic groups, (b) mills, (f) no group, and rotating chains with (c) one, (d) zero, (e) two self-intersections.

theses groups we increased η and at least up to $\eta=1$ these types of shapes form and persist. Noise appears to even stabilise these shapes, or at least make them flow more smoothly. Indeed, in the error-free case, we see some synchronization/clumping within the group after it has formed. This results in the creation of a number of tightly bound subgroups, rather than the particles being randomly or individually positioned throughout the group shape. As e is increased sufficiently this clumping is no longer seen.

The rotating chain structures are not only observed for specific parameter values, nor is there always a unique structure for any given set of parameter values. Fig. 6 shows the group alignment as a function d for fixed $c=1$ in a situation with blind angle and noise of both types. As d increases from 0 to 4 we observe well-defined peaks in the alignment profile. Comparing the collective structures to the observed alignment measure we see that for low directional inertia ($d<0.7$) one or more small highly aligned groups (similar to those in Fig. 4) form, producing a high degree of alignment. For intermediate directional inertia ($0.7<d<2.6$) it is usually mills which form, although for $d>1.7$ rotating chains with one intersection point occasionally form. Between $2.6<d<3.6$ single intersection chains are the most common outcome, but while $2.6<d<3.1$ the 0 and 2 intersection chains with low alignment are also a stable outcome. For $d>3.6$ rotating chains become increasingly rare and usually no group (low alignment) is formed.

4. Discussion

Self-propelled particle models based on attraction alone can produce a large set of collective patterns. Without a blind angle, both undirected mills and moving dynamic groups were possible. The existence of an undirected mill in continuous time follows from a result in classical mechanics of circular motion, see e.g. Young and Freedman (2007). In the continuous version of this

model dynamic moving groups are not possible, since as $\delta \to 0$ and R fixed, Eq. (11) gives

$$\frac{R}{2\delta} \to \infty.$$

Typically in our simulations, we choose δ to be an order of magnitude smaller than R and thus the patterns we observe are not an unrealistic artefact of discrete updating. Indeed, in the context of collective animal behaviour it is biologically realistic to assume a finite interaction radius and discrete directional updates. In doing so, we attempt to model an individual cycle of observe-assess-act in each time step, and find that this alone can generate collective patterns.

The addition of a blind angle causes undirected mills to become at least partially directed. Even more striking is that a blind angle produces collectively moving groups with internal motion. The rotating chains move largely in the same direction while exhibiting a high degree of internal dynamics. Such internal dynamics are regularly observed in bird flocks (Ballerini et al., 2008) and fish schools, but are not generally seen in self-propelled particle models based on alignment terms (Aoki, 1982; Huth and Wissel, 1991; Vicsek et al., 1995; Grégorie et al., 2003; Czirók et al., 1997, 1999; Couzin et al., 2002; D'Orsogna et al., 2006; Wood and Ackland, 2007). We would go as far as to say that in our model the alignment term inhibits internal dynamics within a group. We have run simulations which include a small alignment term and this appears to promote aligned groups which look like those in Fig. 4b to such a degree that the more interesting shapes of Fig. 5 are prevented from forming (results not shown here).

Using the probability of updating scheme on the one self-intersection structure we get groups that look less synthetic but still have the same mode of motion (see video 4). As decreasing p allow us to lower δ to very small values relative to the size of the group structure it seems likely that groups of this type can persist in the presence of a suitable close range repulsion interaction. These groups are less stable than the typical one as particles may on occasion stray from the group.

In the non-blind angle case the interaction in the final groups are always almost global. That is, the size of the group is less than or on par with the interaction radius R. In the blind angle case we observe final groups where the interaction is truly local. On average each particle in the group in Fig. 5(c) is in contact with 40% of the other particles and the interaction radius R is slightly more than half the (largest) width of the shape. By lowering R and increasing β one can produce more exotic rotating chains with one self-intersection in which the degree of contact is as low as 25%. Zero self-intersecting rotating chains have similar contact characteristics and the doubly intersecting ones typically have a lower degree of contact.

Local interaction is not a necessary requirement for one self-intersecting rotating chains to form. In the global attraction model a one self-intersecting rotating chain, there called a dumb-bell, has been observed and discussed (Ebeling and Schimansky-Geier, 2008). Unfortunately a detailed direct comparison of the models is complicated due to the continuous distance dependence of the interaction in the global case. However, connecting the two models will likely provide insight into the nature of the rotating chains as well as requirements for their existence. So future work will involve constructing and analysing a model containing the global, the localised global and the one presented in this paper as special cases.

In the error-free case the particles clump together in subgroups within the original group shape. However, in more realistic situations with angular noise added this does not occur and the groups appear visually less synthetic. These group structures not only persist under angular noise but also if the

speed of each individual is allowed to vary randomly within a certain range. The fact that these groups are generated by simple natural rules, exhibit collective motion with internal motion and persist, or rather are perfected, by angular noise and heterogeneity in speed make them highly relevant for experimental investigation. Several research projects are now looking at the rules of motion followed by individual animals within a group (Ballerini et al., 2008; Nagy et al., 2010). Our contention is that an initial focus on between individual attraction could prove a valuable starting point.

The first part of this paper shows that with simple mathematical reasoning one can obtain reliable information about reasonably complex collective structures. Our mathematical understanding of why the introduction of a blind angle admit the formation of rotating chains and seem to promote orientation in general is weak. Answering these two questions and understanding what type of groups form for different parameter values, as we did in the non-blind angle case, are the primary goals of our present and future work on this model. The find that only attraction to the centre of mass and a blind angle typically produce totally aligned string-like groups like those termed *packs* in Wood and Ackland (2007) might provide a suitable starting point for such an analysis.

Acknowledgements

Appendix A

For a particle moving with constant speed δ on a circle of radius r the angle between previous and current heading φ_c must be

$$\varphi_c = 2\arcsin\left(\frac{\delta}{2r}\right).$$

To see this consider Fig. A1. From elementary geometry we know that

$$\delta = 2r\sin\left(\frac{\alpha}{2}\right),$$

so

$$\alpha = 2\arcsin\left(\frac{\delta}{2r}\right).$$

Furthermore we have that

$$\pi = \varphi_c + 2\varphi_{CM} = \alpha + 2\varphi_{CM},$$

so $\varphi_c = \alpha$ and thus

$$\varphi_c = 2\arcsin\left(\frac{\delta}{2r}\right). \tag{A.1}$$

In order to find an expression for φ_c in terms of the model parameters we need to find the circle radius r in terms of c, d and δ. Consider Fig. 1. The heading of the particle is determined by

$$\tilde{\delta}_t = c\hat{C}_t + d\hat{D}_t,$$

and this vector is then scaled by a number k to make its length δ,

$$\overline{\delta}_t = k\tilde{\delta}_t \quad \text{with} \quad k = \frac{\delta}{|\tilde{\delta}_t|}.$$
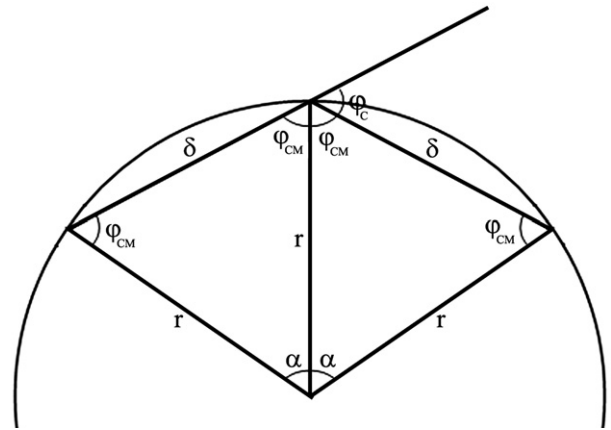

Fig. A1. Part of Fig. 1 highlighting the geometry needed to obtain an expression for the angle φ_c in terms of the radius r of the circle and speed δ of the particle.
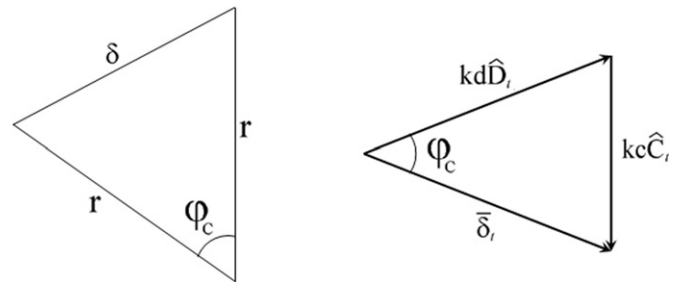

Fig. A2. These two triangles from Fig. 1 are similar and thus we can derive an expression for the radius of the circle in terms of c, d and δ.

Hence

$$\overline{\delta}_t = kc\hat{C}_t + kd\hat{D}_t.$$

Also, the geometry forces $|\overline{\delta}_t| = |kd\hat{D}_t|$ so the triangles in Fig. A2 are similar and, therefore, we have that

$$\frac{|kd\hat{D}_t|}{r} = \frac{|kc\hat{C}_t|}{\delta},$$

$$\frac{kd|\hat{D}_t|}{r} = \frac{kc|\hat{C}_t|}{\delta},$$

$$\frac{d}{r} = \frac{c}{\delta}.$$

Solving this for c gives Eq. (5) and solving for r results in

$$r = \frac{d\delta}{c}. \tag{A.2}$$

Now, combining (A.1) and (A.2) we get (8), that is

$$\varphi_c = 2\arcsin\left(\frac{c}{2d}\right). \tag{A.3}$$

Appendix B. Supplementary material

Supplementary data associated with this article can be found in the online version of 10.1016/j.jtbi.2011.05.019.

References

Aoki, I., 1982. A simulation study on the schooling mechanism in fish. Bulletin of the Japanese Society of Fisheries 48.

Ballerini, M., Cabibbo, N., Candelier, R., Cavagna, A., Cisbani, E., Giardina, I., Orlandi, A., Parisi, G., Procaccini, A., Viale, M., Zdravkovic, V., 2008. Empirical investigation of starling flocks: a benchmark study in collective animal behaviour. Animal Behaviour 76 (1), 201–215.

Bando, M., Hasebe, K., Nakayama, A., Shibata, A., Sugiyama, Y., 1995. Dynamical model of traffic congestion and numerical simulation. Physical Review E 51 (2), 1035–1042.

Bazazi, S., Buhl, J., Hale, J.J., Anstey, M.L., Sword, G.A., Simpson, S.J., Couzin, I.D., 2008. Collective motion and cannibalism in locust migratory bands. Current Biology 18 (10), 735–739.

Buhl, J., Sumpter, D.J.T., Couzin, I.D., Hale, J.J., Despland, E., Miller, E.R., Simpson, S.J., 2006. From disorder to order in marching locusts. Science 312, 1402–1406.

Couzin, I.D., Krause, J., James, R., Ruxtony, G.D., Franks, N.R., 2002. Collective memory and spatial sorting in animal groups. Journal of Theoretical Biology 218, 1–11.

Czirók, A., Vicsek, T., 2000. Collective behavior of interacting self-propelled particles. Physica A 281, 17–29.

Czirók, A., Stanley, H.E., Vicsek, T., 1997. Spontaneously ordered motion of self-propelled particles. Journal of Physica A 30, 1375–1385.

Czirók, A., Vicsek, M., Vicsek, T., 1999. Collective motion of organisms in three dimensions. Physica A 264 (1–2), 299–304.

D'Orsogna, M.R., Chuang, Y.L., Bertozzi, A.L., Chayes, L.S., 2006. Self-propelled particles with soft-core interactions: patterns, stability and collapse. Physical Review Letters 96 (10).

Ebeling, W., Schimansky-Geier, L., 2008. Swarm dynamics, attractors and bifurcations of active Brownian motion. European Physical Journal Special Topics 157, 17–31.

Erdmann, U., Ebeling, W., Mikhailov, A.S., 2005. Noise-induced transition from translational to rotational motion of swarms. Physical Review E 71.

Grégorie, G., Chaté, H., Tu, Y., 2003. Moving and staying together without a leader. Physica D 181.

Hale, J.J., 2008. Automated Tracking and Collective Behaviour in Locusts and Humans. Ph.D. Thesis. University of Oxford.

Huth, A., Wissel, C., 1991. The simulation of the movement of fish schools. Journal of Theoretical Biology 156, 365–385.

Lukeman, R., Li, X.Y., Edelstein-Keshet, L., 2009. A conceptual model formilling formations in biological aggregates. Bulletin of Mathematical Biology 71, 352–382. doi:10.1007/s11538-008-9365-7.

Mikhailov, A.S., Zanette, D.H., 1999. Noise-induced breakdown of coherent collective motion in swarms. Physical Review E 60 (4).

Nagy, M., Ákos, Z., Biro, D., Vicsek, T., 2010. Hierarchical group dynamics in pigeon flocks. Nature 464, 890–893.

Partridge, B.L., 1981. Internal dynamics and the interrelations of fish in schools. Journal of Comparative Physiology 144, 313–325.

Partridge, B.L., Pitcher, T.J., 1980. The sensory basis of fish schools: relative roles of lateral line and vision. Journal of Comparative Physiology 135, 315–325.

Romanczuk, P., Couzin, I.D., Schimansky-Geier, L., 2008. Collective motion due to individual escape and pursuit response. Physical Review Letters 102 (1).

Sugiyama, Y., 2008. Group Formation of Self-driven System. Application of 2-Dimensional Optimal Velocity Model, Presentation Sapporo, September 2008.

Szabó, B., Szöllösi, G.J., Gönci, B., Jurányi, Zs., Selmeczi, D., Vicsek, T., 2006. Phase transition in the collective migration of tissue cells: experiment and model. Physical Review E 74.

Vicsek, T., Czirók, A., Ben-Jacob, E., Cohen, I., Shochet, 0., 1995. Novel type of phase transition in a system of self-driven particles. Physical Review Letters 75 (6), 1226–1229.

Wood, A.J., Ackland, G.J., 2007. Evolving the selfish herd: emergence of distinct aggregating strategies in an individual-based model. Proceedings of Royal Society B 274, 1637–1642.

Yates, C.A., Baker, R., Erban, R., Maini, P., 2010. Refining self-propelled particle models for collective behaviour. Canadian Applied Mathematics Quarterly 18 (3).

Young, H.D., Freedman, R.A., 2007. University Physics with Modern Physics, 12th ed. Addison Wesley.